The Chandra ACIS Survey of M33 (ChASeM33): Investigating the Hot Ionized Medium of NGC604

R. Tüllmann[1], T. J. Gaetz[1], P. P. Plucinsky[1], P. Ghavamian[2], D. Breitschwerdt[3], M. Avillez[4], W. P. Blair[2], K. S. Long[5], T. G. Pannuti[6], P. Frank Winkler[7]

[1]Center for Astrophysics, Harvard University; [2] Dep. of Physics & Astronomy, Johns Hopkins University; [3] Institut für Astronomie, Universität Wien, Austria; [4] Dept. of Mathematics, University of Évora, Portugal; [5] Space Telescope Science Insitute, Baltimore; [6] Space Science Center, Morehead State University; [7] Dept. of Physics, Middlebury College, Middlebury

1. Introduction

We present ongoing results from the Chandra ACIS Survey of M33 (ChASeM33), a 1.4Ms deep survey to investigate the small and large-scale distribution of the Hot Ionized Medium (HIM), the source populations that shape it, and their mutual interaction. ChASeM33 (Plucinsky et al., 2007, astro-ph/0709.4211) provides the highest angular resolution yet achievable in X-ray astronomy (1") and has a limiting luminosity (absorbed) for point sources of 1.6e35 erg/s (0.35-8.0keV bandpass).

In this study we focus on the diffuse extended X-ray emission from NGC604, the largest giant HII-region in M33. The multi-energy band X-ray imaging presented here is the deepest obtained to date of NGC604 (300ks) and reveals an unprecedented level of detail.

We also show the first X-ray spectra of the diffuse emission (0.35-2.0keV) which allow us to constrain fundamental parameters of the ISM, such as gas temperatures, densities, and filling factors.

2. Results

The most striking results concern the spatial extent of the soft X-ray emission and the remarkably good morphological anti-correlation between the emission originating at soft X-rays and Hα (see Fig. 1).

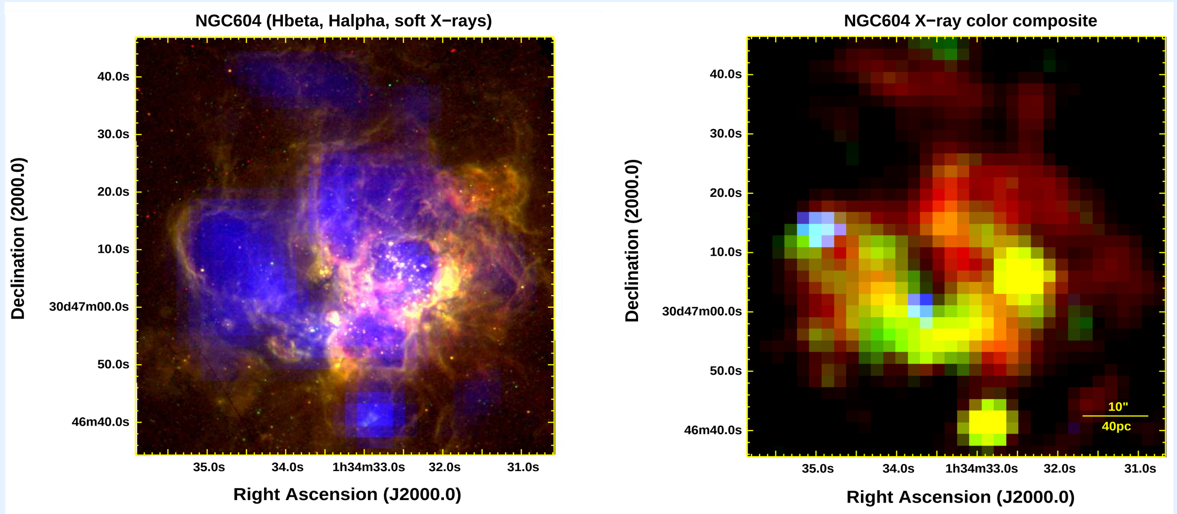

Fig. 1: Left panel: Morphological anti-correlation between Hβ (red), Hα (green), and soft X-rays (0.35 - 1.1 keV, blue). **Right panel:** Three color high resolution (2″) Chandra X-ray image (red: 0.35 – 1.1 keV, green: 1.1 – 2.6 keV, blue: 2.6 – 8.0 keV).

The soft X-ray emission is much more extended along the N-S axis of NGC604 than previous measurements indicate, reaching 90% (= 372 pc) of the extent of the Hα-emitting gas.

Figs. 1, 3, and 4 show that all cavities (C1-C3) and bubbles (B1-B3) are filled with hot gas (see Fig. 5 for their locations).

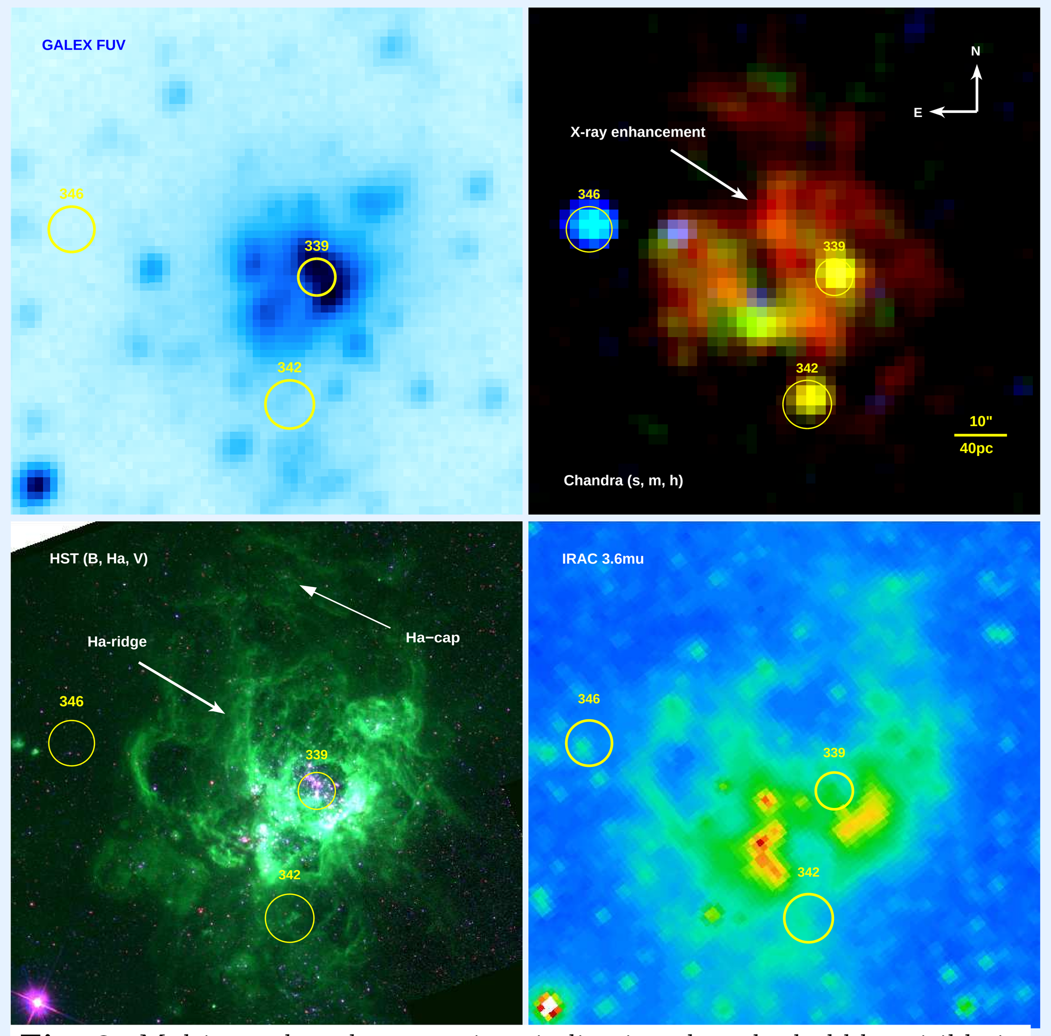

Fig. 2: Multi-wavelength comparison indicating that the bubbles visible in Hα are filled with X-ray-hot gas and are powered by the central OB/WR-stars. Yellow circles represent detected Chandra point sources (taken from the ChASeM33 point source catalog (Plucinsky et al. 2007)).

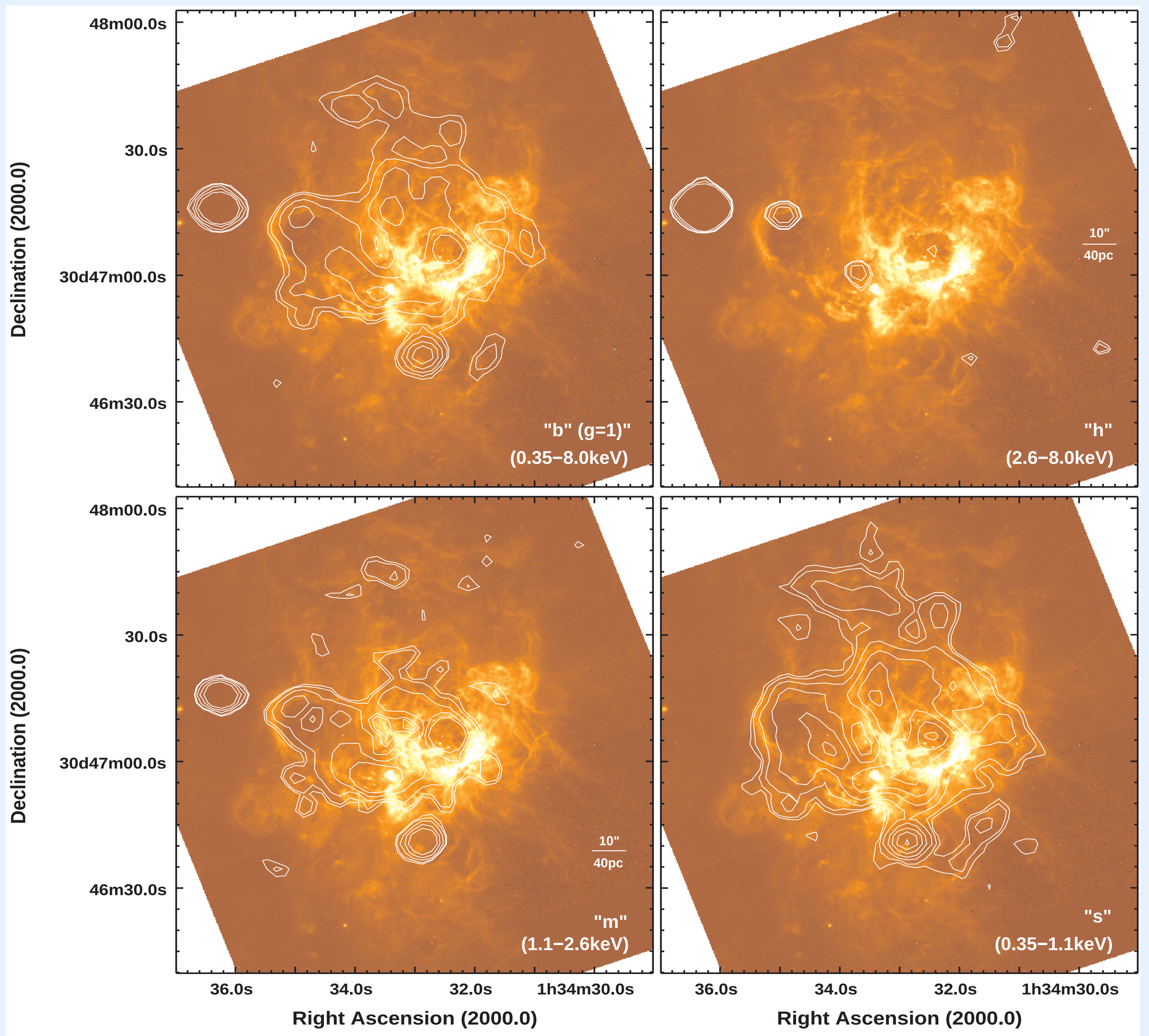

Fig. 3: ACIS-I contour maps are smoothed with a Gaussian filter of FWHM = 2.0" and are overlaid onto a HST-Hα-image of NGC 604.

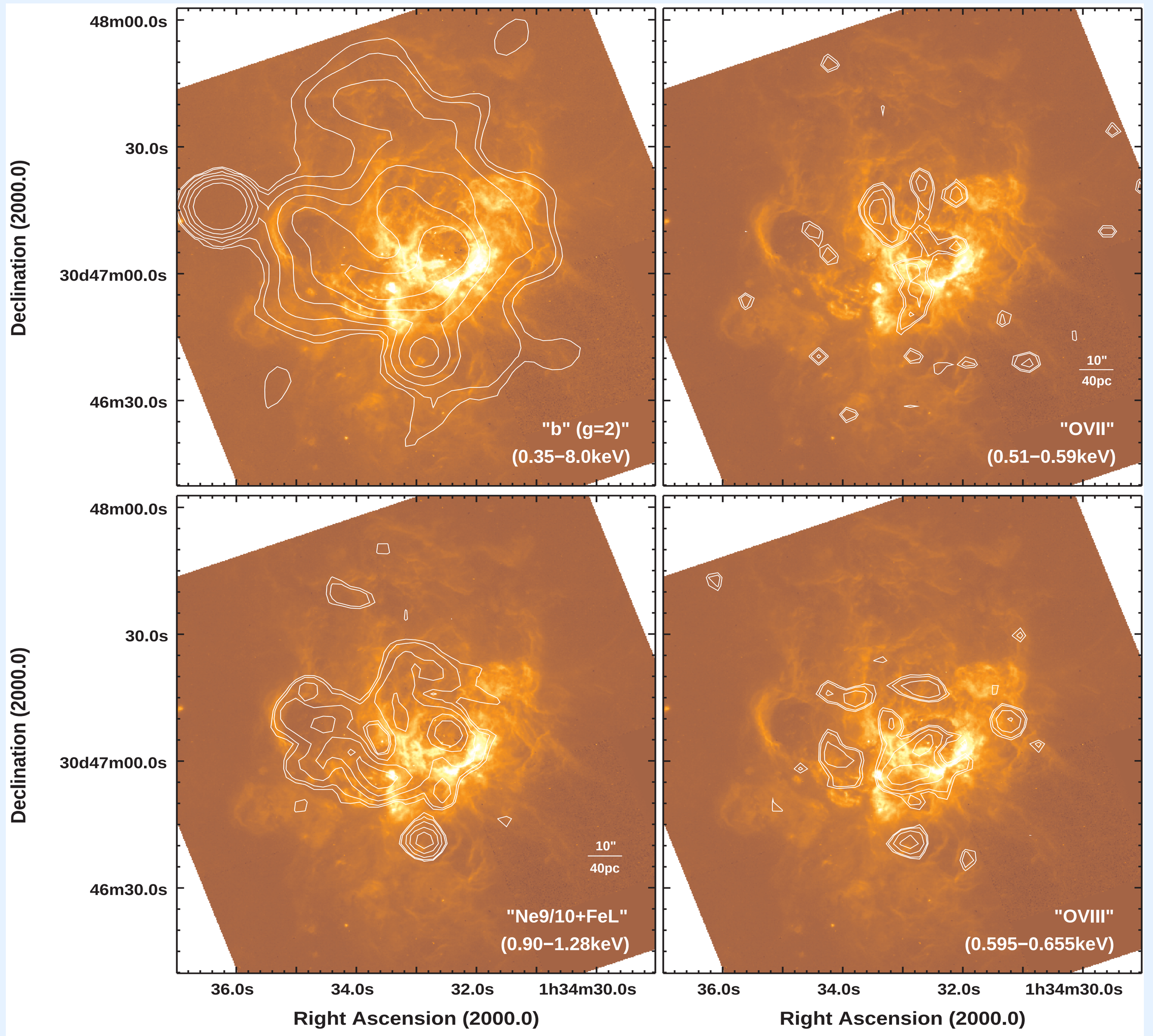

Fig. 4: The "broad"-contour map (upper left) has been smoothed with a Gaussian filter of 4" to highlight the overall extent of the X-ray emission.

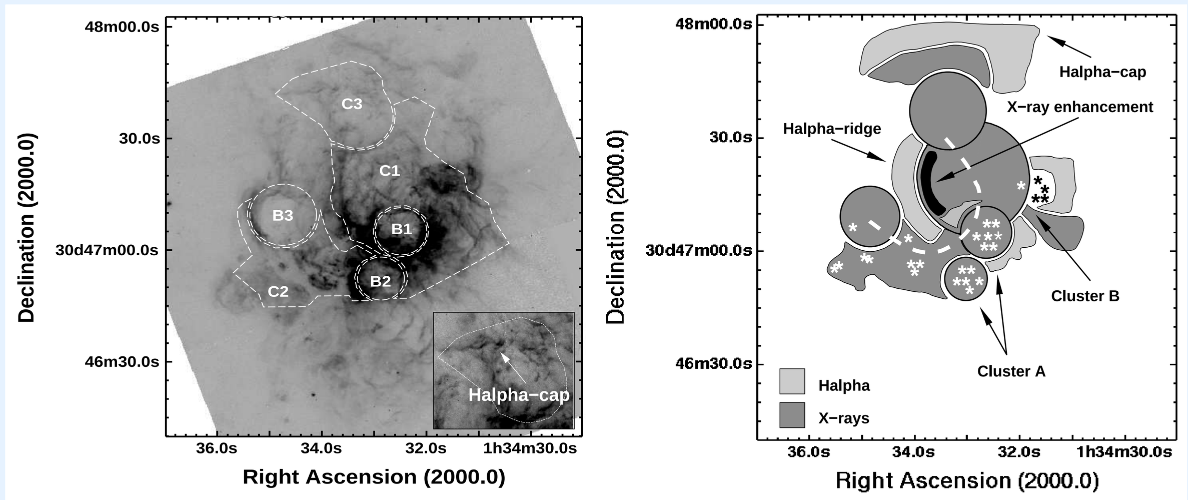

Fig. 5: Left panel: Spectral extracion regions. Right panel: Sketch of NGC604.

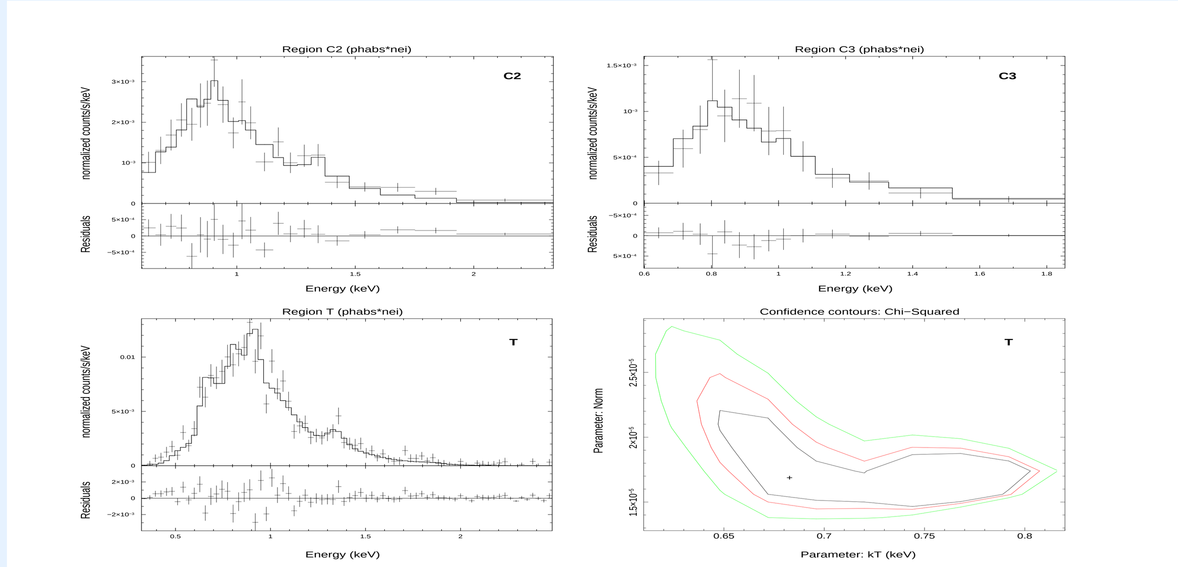

Fig. 6: Spectra extracted from regions shown in Fig. 5 cover the range from 0.35 - 2.5 keV. 90%-confidence contours are plotted for the total diffuse emission (label 'T').

Table 1: Derived physical parameters

Region	kT	$F_{X,abs}$	$F_{X,unabs}$	$L_{X,unabs}$	V	M_X	n_e (cm^{-3})		
	keV	10^{-14} erg s^{-1} cm^{-2}		10^{35} erg s^{-1}	10^{60} cm^3	$M_\odot$	f_X		
(1)	(2)	(3)	(4)	(5)	(6)	(7)	0.1	0.5	0.8
C1	0.325±0.075	1.68±0.32	2.27±0.32	4.52±0.72	12.5±6.98	757±51	0.33	0.15	0.12
C2	0.810±0.095	0.98±0.92	1.23±0.92	2.45±1.83	3.62±0.77	195±85	0.29	0.13	0.10
C3	0.567±0.145	0.33±0.13	0.45±0.13	0.90±0.26	4.85±1.45	294±135	0.18	0.08	0.06
B1	0.616±0.168	0.25±0.08	0.31±0.08	0.62±0.16	1.40±0.14	85±28	0.27	0.12	0.09
B2	0.536±0.209	0.38±0.16	0.54±0.16	1.08±0.32	0.88±0.08	71±18	0.33	0.15	0.12
B3	0.685±0.168	0.47±0.16	0.59±0.16	1.18±0.32	3.17±0.32	171±64	0.23	0.11	0.08
T	0.683±0.016	3.74±0.36	5.32±0.36	10.6±0.72	26.4±0.72	1422±182	0.23	0.10	0.08

Notes: Col. (1): All spectra were extracted from eventlists cleaned from point sources to trace the pure diffuse emission. Cols. (2): Plasma temperatures are derived using `Xspec` and a (*phabs* × *nei*)-model (Borkowski et al. 2001) and freezing the neutral hydrogen column density at $N_H = 5.21 \times 10^{20}$ cm^{-3} (Gonzalez-Delgado & Pérez 2000). A conversion from (keV) → (K) is achieved, using T (K) $= 1.16 \times 10^7 kT$ (keV), with kT being the energy of a thermal source. Cols (3) and (4): Absorbed and unabsorbed fluxes are listed for the 0.35 – 2.0 keV energy band. All uncertainties are given on a 90%-confidence level using the `error` command in `XSPEC`. Col. (5): X-ray luminosities between 0.35 – 2.0 keV assume a distance to M33 of $D = 817$ kpc (Freedman et al. 2001). Cols (6) – (7): Estimated volume and X-ray gas mass. M_X is based on the electron density obtained if a filling factor of $f_X = 0.8$ is adopted.

A morphological comparison between X-ray, FUV, optical, and FIR emission (see Fig. 2) suggests that the bubbles and cavities visible in Hα are powered by the massive OB and WR-star associations in the center of NGC 604.

The diffuse X-ray emission (Fig. 6) can be well fitted with a 2-component model consisting of a photoelectric absorber (phabs) and a thermal plasma (nei).

3. Conclusions

- The Hα-emitting gas seems to confine the X-ray gas which implies a high filling factor for the HIM. Adopting $f_X = 0.8$, yields $n_e \leq 0.1\,\mathrm{cm}^{-3}$ (cf. Table 1).
- X-ray luminosities and gas masses in the main cavity (B1+B2+C1+C3) are consistent with stellar mass loss from ∼ 200 O/WR-type stars (including evaporation from thermal heat conduction).
- The X-ray-enhancement visible in cavity C1 (Fig. 2) can likely be attributed to a stellar wind which got hit by a reverse shock after it impinged onto the Hα-ridge.
- As the high-pressure wind-driven X-ray gas is able to penetrate the whole volume it seems plausible to assume break-out of hot gas on large scales.

This work is supported by NASA Chandra award number GO6-7073A.